Research Article | Vol. 26, No. 18 | 3 Sep 2018 | OPTICS EXPRESS 22761
Optics EXPRESS

Polarization-insensitive phase conjugation using single pump Bragg-scattering four-wave mixing in semiconductor optical amplifiers

ANEESH SOBHANAN AND DEEPA VENKITESH*

Dept. of Electrical Engineering, Indian Institute of Technology Madras, Chennai 600036, India
**deepa@ee.iitm.ac.in*

Abstract: We explain the generation of four wave mixing (FWM) components at the front and back facets of semiconductor optical amplifiers (SOAs) based on the Bragg-scattering from the propagating gratings in the SOAs. We propose a counter-propagating cross-polarized degenerate pumping scheme for polarization-insensitive conjugate generation, simultaneously in both input and output ports of the SOA for the first time. The corresponding Bragg scattering processes along with the phase matching conditions are described and the detuning performance of the generated conjugate in either port are experimentally validated. Polarization-insensitive phase conjugate generation at both input and output ports of the SOA through Bragg scattering FWM is further demonstrated.

1. Introduction

All-optical chromatic dispersion compensation and nonlinearity mitigation using phase conjugation are attracting renewed attention with the advent of advanced modulation formats in optical communication [1, 2]. Four-wave mixing (FWM) in nonlinear media such as highly nonlinear fiber (HNLF) and nonlinear semiconductor optical amplifier (SOA) is typically utilized to achieve phase conjugation. Of these, SOAs are particularly attractive because of its smaller footprint, potential for photonic integration [3] and increased energy efficiency [4]. Similar to that in HNLF, SOA-based FWM also has the advantage of being impervious to bit-rates and modulation formats. Polarization sensitivity of four-wave mixing process is one of the primary challenges in the implementation of phase conjugation. In an optical network that uses polarization multiplexing, polarization-insensitive FWM scheme is required for practical implementation of phase conjugator. Several research groups have undertaken detailed theoretical studies of polarization-insensitive schemes [5–7]. Four wave mixing-based optical spectral inversion without frequency shift by using two orthogonally polarized pumps in fiber and in SOA are reported in [8,9]. The dependence of wavelength spacing between the pumps and that between the signal and the pump on polarization-insensitive conjugate generation for SOAs is reported in [10]. The use of two-orthogonally polarized pumps in a polarization diversity scheme is experimentally demonstrated in [11]. Further, the operating principle of the polarization-insensitive FWM is analyzed using an improved space-averaged model and a comparative study of efficiencies among different pump polarization configurations is undertaken using a model by KA Shore's group [12–18]. A scheme with the probe and conjugate waves propagating in opposite directions in SOA using counter-propagating orthogonally polarized pumps was demonstrated in [19] while phase conjugation using counter-propagating non-degenerate pumps was recently demonstrated in [20]. In both these demonstrations, pump and probe are generated in one port while pump and conjugate are generated at the second port of the SOA.

Though conjugate generation in the bidirectional pumping scheme in SOA has been studied in the past, a detailed analysis of the mechanism of generation of conjugates in either port of SOA, their corresponding phase matching conditions and polarization states have not been discussed. We propose the Bragg-scattering theory to explain the generation of conjugates, that are insensitive

#334659 https://doi.org/10.1364/OE.26.022761
Journal © 2018 Received 7 Jun 2018; revised 24 Jul 2018; accepted 24 Jul 2018; published 21 Aug 2018
Corrected: 05 September 2018

to the polarization of the input signal in both the ports of an SOA simultaneously, in a partially degenerate FWM configuration. Experiments on FWM initiated through Bragg-scattering (FWM-BS) have been demonstrated by many research groups in the past using other nonlinear media such as highly nonlinear fiber, birefringent photonic crystal fiber, silica and photonic band-gap fiber [21–25]. In this paper, we discuss the details of FWM initiated through Bragg scattering in SOAs for the first time. We explain the direction of propagation of the conjugates by accounting for the facet reflectivities in SOAs as evidenced by our previous experimental observations in [26]. We further perform experiments with degenerate pumps that are counter propagating in the SOA with cross polarization and demonstrate polarization-insensitive phase conjugate generation in both input and output ports of SOA. We also establish the corresponding detuning characteristics in both the ports.

2. Theory

The nature of Bragg scattering-based four wave mixing in SOAs is influenced by the structure of the SOA. Even though SOAs are designed to be traveling wave structures, the non-zero facet reflectivity influences the four wave mixing process. The facet reflectivity of a given SOA can be experimentally measured from the amplified spontaneous emission (ASE) spectrum [27].

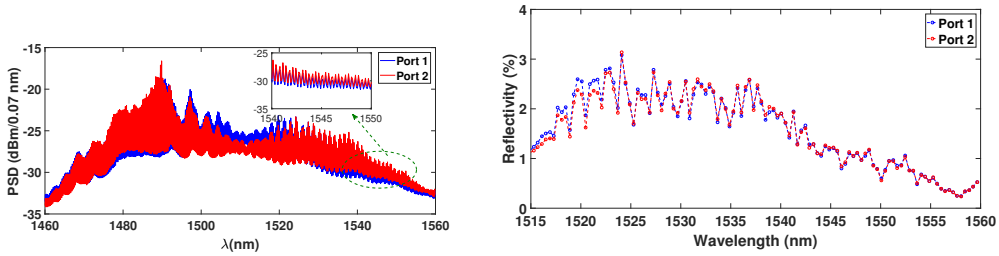

(a) (b)

Fig. 1. (a) Power spectral density of amplified spontaneous emission spectra observed at the input and output ports of SOA for a drive current of 375 mA. The ASE near 1545 nm is zoomed and shown in inset, (b) Reflectivity spectra of the SOA at both port 1 and port 2 for a drive current of 375 mA

Figure. 1(a) shows the ASE spectra of the SOA (SOA-NL-L1-C-FA; Kamelian, with a saturation output power ≈ 11.5 dBm for a drive current of 375 mA, a polarization dependent gain of 1 dB and gain recovery time of 25 ps) used in our experiments, measured at its input and output ports (referred to as port 1 and port 2 respectively). The presence of facet reflections is evidenced by the stable and equi-spaced spectral lines, similar to that from the output of a Fabry-Perot resonator. The frequency spacing is observed to be 50 GHz, corresponding to a device length of ∼1 mm. The facet reflectivities can be estimated from the ASE spectra using conventional Hakki-Paoli's relation between the depth of the gain-ripple, facet reflectivity and the single pass gain (G_s) [27]. This relation is given as,

$$R(\%) = \frac{1}{G_s}\left[\frac{(P^+)^{1/2} - (P^-)^{1/2}}{(P^+)^{1/2} + (P^-)^{1/2}}\right] \times 100, \tag{1}$$

where R represents the geometrical mean of the facet reflectivities of either end; P^+ and P^- represent the maximum and minimum power levels respectively, measured from the ASE spectra. The reflectivities calculated across the C-band for the SOAs used in our experiment is shown in Fig. 1(b). Note that the calculation shown above uses $G_s = 10\ dB$ (fiber-to-fiber gain from the data sheet) and does not include the fiber-to-chip-to-fiber insertion loss of the SOA since such

information is not available to us. If this is also included, the reflectivity would further decrease by the same factor as the insertion loss. However, the theory discussed below is not dependent on the exact value of reflectivity but relies on the fact that the reflectivity is *non-zero*. Even though the magnitude of reflectivity is small, the reflected power experiences gain in the SOA which is sufficient to contribute to the formation of gratings, as evidenced by the experimental results discussed in Section 3.

Note that the ASE spectra measured in either port are almost identical for a given drive current, as indicated in Fig. 1(a). Considering the facet reflectivity, we now discuss the direction of propagation of moving grating generated due to the beat between the pump and signal (with frequencies ω_p and ω_s respectively), and the direction of propagation of the generated idler and conjugate (with frequencies $2\omega_s - \omega_p$ and $2\omega_p - \omega_s$ respectively) in an SOA.

Consider a signal and pump that are co-polarized, which are co-propagating in a nonlinear SOA in the partially degenerate scheme. The co-propagating pump and signal at different optical frequencies (ω_p & ω_s) generate a beat frequency (Ω) in the medium and the carrier density responds to this beat frequency, given as, $\Omega = |\omega_s - \omega_p|$ [28–30]. The modulation of carrier density at this beat frequency results in a gain grating and hence a corresponding refractive index grating at this beat frequency. Thus, in a conventionally described FWM occurring due to population pulsations [28], the pump and signal interacting with this grating generates additional frequency components, corresponding to frequencies $\omega_p \pm \Omega$ and $\omega_s \pm \Omega$. However, in the Bragg scattering process, we consider the propagating gratings due to the detuned signal and pump.

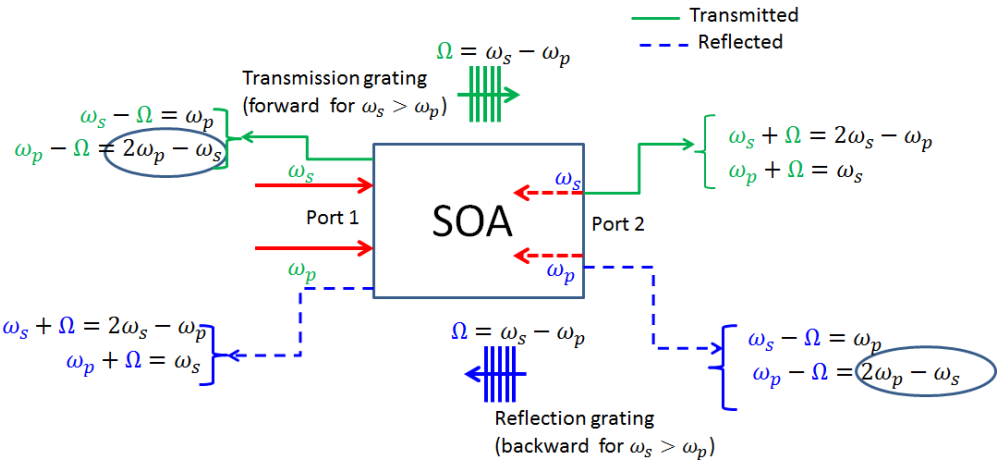

Fig. 2. Schematic of direction of propagation of moving grating and conditions for idler and conjugate generation at the either ports of the SOA, considering facet reflectivity. Co-propagating signal and pump with $\omega_s > \omega_p$ is considered. The reflected frequencies, the generated idler and conjugate due to reflected grating, reflected signal and pumps are shown as broken lines.

The detuning between the signal and the pump and their directions of propagation decide the strength and direction of propagation of the gratings. The schematic of the processes leading to Bragg scattering-based FWM is shown in Fig. 2. The idlers are generated with frequencies based on the corresponding Doppler shift. For instance, Fig. 2 shows the case when pump and signal are launched at port 1 with $\omega_s > \omega_p$, where the generated grating (with period $\Omega = \omega_s - \omega_p$, wave vector $k_s - k_p$) moves in the forward direction. Both the pump and signal gets diffracted off this moving grating and generate idlers corresponding to frequencies (a) $\omega_{s/p} + \Omega$ $(= 2\omega_s - \omega_p/\omega_s)$

Optics EXPRESS

in the forward direction which appears in port 2 and (b) $\omega_{s/p} - \Omega$ $(= \omega_p/2\omega_p - \omega_s)$ in the backward direction, which appears at port 1. Thus in the absence of facet reflectivity, the idler at frequency $2\omega_s - \omega_p$ is not expected to appear at port 1 and the conjugate at frequency $2\omega_p - \omega_s$ is not expected at port 2. However the idler and the conjugate are usually observed at both the ports in an experiment. This can be explained due to the diffractions from the grating generated due to the reflected light from either facets- referred to as the reflection grating. The frequencies generated due to the interaction of reflected grating with the forward propagating pump and signal are shown in Fig. 2, in dotted lines.

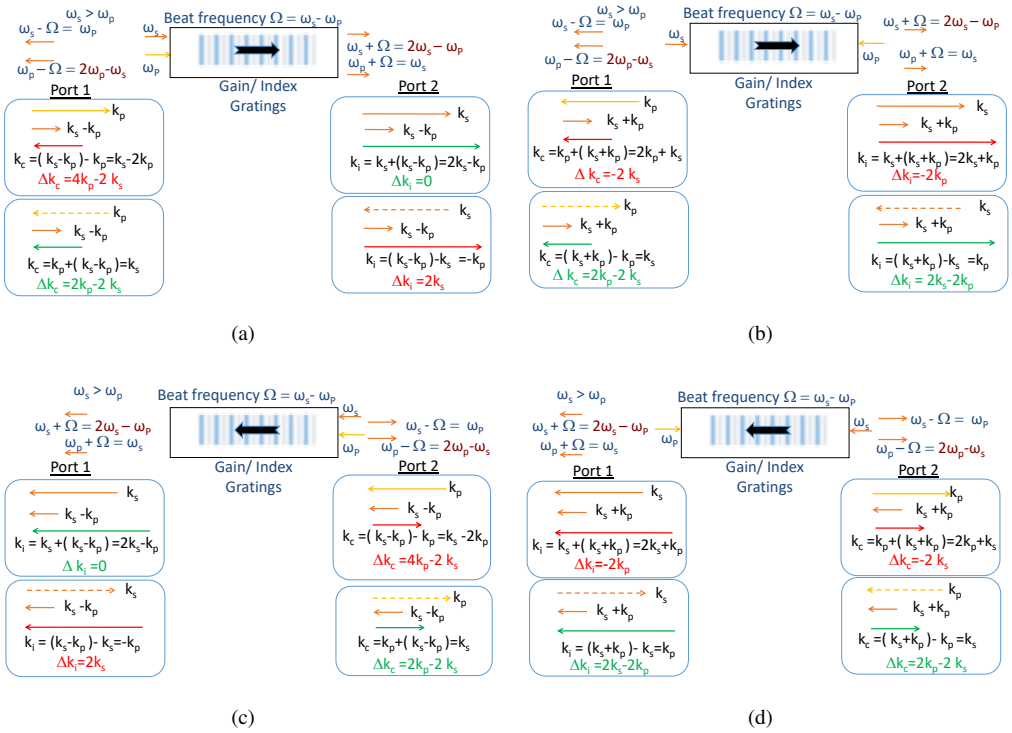

Fig. 3. Forward and backward propagating grating formation and the forbidden (red) and non-forbidden (green) idler/conjugate at port 1 and port 2 of SOA based on phase matching condition for $\omega_s > \omega_p$. The reflected signal and pump from the SOA facets are indicated with the dotted lines. (a) Forward propagating grating formed by the beating between co-propagating signal and pump launched from port1. (b) Forward propagating grating formed by the beating between counter-propagating pump and co-propagating signal. (c) Backward propagating grating formed by the beating between co-propagating signal and pump launched from port 2. (d) Backward propagating grating formed by the beating between counter-propagating signal and co-propagating pump

It must be noted that the scattering from the moving grating also requires phase matching conditions to be satisfied. The wave vectors corresponding to pump, signal, idler/conjugate and the moving grating (k_p, k_s, $k_{i/c}$, and $(k_s - k_p \,/\, k_s + k_p)$) and phase mismatch for each scattering process is shown in Fig. 3. Note that the magnitudes of all the grating vectors are decided by the detuning between the signal and the pump.

The formation of forward and backward propagating gratings and the subsequent generation of additional frequencies are shown separately in Fig. 3. The vector diagram corresponding to the generation of conjugate and idler in each port and the corresponding phase mismatch

is shown in separate boxes. The phase mismatch for the conjugate $\triangle k_c$ is calculated as $\triangle k_c = k_c - (2k_p - k_s)$ and for the idler, $\triangle k_i$ is calculated as $\triangle k_i = k_i - (2k_s - k_p)$ in each case [12]. It is evident that the generation of certain frequencies is forbidden (the corresponding phase matching conditions are indicated in red in Fig. 3). For instance, the interaction of forward propagating pump with the co-propagating grating (with wavevector $k_s - k_p$) leads to a conjugate in port 1 (with wave vector $(k_s - k_p) - k_p = k_s - 2k_p$) with a large phase mismatch given by $\triangle k_c = (2k_p - k_s) - (k_s - 2k_p) = 4k_p - 2k_s$, due to which the conjugate does not get generated in port 1 efficiently due to this interaction. The corresponding vector diagram is shown in the top-left box in Fig. 3(a). However, conjugate generation in port 1 is possible due to the interaction between the reflected pump (indicated with a dotted line in the bottom-left box in Fig. 3(a)) with the same forward propagating grating with a negligible phase mismatch of $2k_p - 2k_s$. Similarly, the conjugate generation in port 2 due to the interaction between counter-propagating pump and backward propagating grating (wave vector $k_s - k_p$) is forbidden; while that due to the interaction between the same backward propagating grating with the reflected pump is allowed as shown in Fig. 3(c). From all possibilities shown in Fig. 3, it is evident that the conjugate generation in both ports 1 and port 2 can be explained only through the Bragg scattering process. The detuning characteristics of conversion efficiency are decided by the corresponding phase matching conditions. The polarization of the generated frequency is identical to that of the field (pump/signal) that interacts with the grating.

Table 1. Frequencies generated in each port of SOA with non-zero facet reflectivity; Positive detuning ($\omega_s > \omega_p$); grating due to co-propagating signal and pump. The signal is assumed to have arbitrary polarization. Pump and signal polarization and direction of propagation are indicated in the first column. Frequencies shown in green satisfy phase matching condition

Interacting frequency	$\omega_s > \omega_p$ (Positive Detuning) Grating Frequency : $(\Omega = \omega_s - \omega_p)$			
	Grating due to co-prop ω_s **&** ω_p **Forward**; Grating vector: $k_s - k_p$		**Grating due to reflected** ω_s **&** ω_p **Backward**; Grating vector: $k_s - k_p$	
	Port 1	Port 2	Port 1	Port 2
ω_p (co-prop)- $\parallel$	$2\omega_p - \omega_s$	ω_s	ω_s	$2\omega_p - \omega_s$ $(\parallel)$
ω_p (reflected)- $\perp$	$2\omega_p - \omega_s$	ω_s	ω_s	$2\omega_p - \omega_s$ $(\perp)$
ω_p (counter-prop)- $\perp$	$2\omega_p - \omega_s$ $(\perp)$	ω_s	ω_s	$2\omega_p - \omega_s$
ω_p (reflected)- $\parallel$	$2\omega_p - \omega_s$ $(\parallel)$	ω_s	ω_s	$2\omega_p - \omega_s$
ω_s (co-prop)- $\parallel + \perp$	ω_p	$2\omega_s - \omega_p$	$2\omega_s - \omega_p$	ω_p
ω_s (reflected)- $\parallel + \perp$	ω_p	$2\omega_s - \omega_p$	$2\omega_s - \omega_p$	ω_p

The Bragg-scattering process discussed above assumes co-polarized pump and signal. Polarization-insensitive conjugate generation is achieved through counter-propagating orthogonal pumps. The signal is assumed to be arbitrarily polarized. The mechanism of grating formation and the generation of idler and conjugate at specific ports can be analyzed based on the Bragg-scattering process discussed above and phase matching conditions discussed in Fig. 3. The possible frequencies and the ports at which they are generated are given in Tables. 1, 2, 3 and 4. The possibilities including the case where $\omega_p > \omega_s$ are also tabulated; forbidden processes are

marked in red and allowed processes are marked in green. The orthogonal polarizations parallel and perpendicular (X-pol and Y-pol) are marked as $\parallel$ and $\perp$ in the Tables. The phase matching conditions worked out in these tables are for the case where the incident pump in the forward direction has $\parallel$ polarization and that counter-propagating through the SOA has $\perp$ polarization.

From Table.1, it is evident that the polarization-insensitive conjugate generation occurs at port 1 (which are marked as green) from scattering off counter propagating pump ($\perp$) and the reflected pump ($\parallel$) from the forward propagating grating (generated due to co-propagating signal and pump). There is an additional contribution to the generation of the conjugate in both polarizations in port 1 due to the interaction of forward pump ($\parallel$) and reflected pump ($\perp$) with forward propagating grating generated due to co-propagating signal and counter-propagating pump (with wavevector $k_s + k_p$) as shown in Table. 2. Similarly, we can explain the polarization-insensitive phase conjugate generation in port 2 of SOA as well. From Table. 2 it is seen that the scattering of counter propagating pump ($\perp$) and the reflected pump ($\parallel$) off the backward propagating grating (formed due to reflected signal and co-propagating pump) results in a polarization-insensitive phase conjugation. Similar to that in port 1, an additional contribution of the conjugate in $\parallel$ and $\perp$ polarization is generated in port 2 due to the interaction of forward pump ($\parallel$) and reflected pump ($\perp$) respectively, with backward propagating grating due to reflected signal and counter-propagating pump (as shown in Table. 1).

Table 2. Frequencies generated in each port of SOA with non-zero facet reflectivity; Positive detuning ($\omega_s > \omega_p$); grating due to counter-propagating signal and pump. The signal is assumed to have arbitrary polarization.Frequencies shown in green satisfy phase matching condition.

Interacting frequency	$\omega_s > \omega_p$ (Positive Detuning) Grating Frequency : $(\Omega = \omega_s - \omega_p)$			
	Grating due to co-prop ω_s & counter propagating ω_p **Forward**; Grating vector: $k_s + k_p$		**Grating due to reflected ω_s & co-propagating ω_p** **Backward**; Grating vector: $k_s + k_p$	
	Port 1	Port 2	Port 1	Port 2
ω_p (co-prop)- $\parallel$	$2\omega_p - \omega_s$ $(\parallel)$	ω_s	ω_s	$2\omega_p - \omega_s$
ω_p (reflected)- $\perp$	$2\omega_p - \omega_s$ $(\perp)$	ω_s	ω_s	$2\omega_p - \omega_s$
ω_p (counter-prop)- $\perp$	$2\omega_p - \omega_s$	ω_s	ω_s	$2\omega_p - \omega_s$ $(\perp)$
ω_p (reflected)- $\parallel$	$2\omega_p - \omega_s$	ω_s	ω_s	$2\omega_p - \omega_s$ $(\parallel)$
ω_s (co-prop)- $\parallel + \perp$	ω_p	$2\omega_s - \omega_p$	$2\omega_s - \omega_p$	ω_p
ω_s (reflected)- $\parallel + \perp$	ω_p	$2\omega_s - \omega_p$	$2\omega_s - \omega_p$	ω_p

Tables 1 and 2 explain the polarization-insensitive phase conjugate generation in both the ports of SOA for positive detuning ($\omega_s > \omega_p$). Similarly, we can deduce the corresponding Bragg-scattering processes for negative detuning ($\omega_p > \omega_s$) (given in appendix A), and these are shown in Tables 3 and 4. It is evident that polarization-insensitive conjugate generation is possible in either port even for negative detuning. The predominant contributor to polarization-insensitive conjugate generation in port 1 in this case is due to the grating formed by the reflected signal

Optics EXPRESS

Table 3. Frequencies generated in each port for cross-polarized and counter propagating pumps, $\omega_p > \omega_s$; grating due to co-propagating signal and pump. The signal is assumed to have arbitrary polarization. Frequencies shown in green satisfy phase matching condition.

	Grating due to co-prop ω_s & ω_p **Forward**: Grating vector: $k_p - k_s$		**Grating due to reflected ω_s & ω_p** **Backward**: Grating vector: $k_p - k_s$	
	Port 1	Port 2	Port 1	Port 2
ω_p (co-prop)-$\parallel$	ω_s	$2\omega_p - \omega_s$ ($\parallel$)	$2\omega_p - \omega_s$	ω_s
ω_p (reflected)-$\perp$	ω_s	$2\omega_p - \omega_s$ ($\perp$)	$2\omega_p - \omega_s$	ω_s
ω_p (counter-prop)- $\perp$	ω_s	$2\omega_p - \omega_s$	$2\omega_p - \omega_s$ ($\perp$)	ω_s
ω_p (reflected)- $\parallel$	ω_s	$2\omega_p - \omega_s$	$2\omega_p - \omega_s$ ($\parallel$)	ω_s
ω_s (co-prop)- $\perp$ + $\parallel$	$2\omega_s - \omega_p$	ω_p	ω_p	$2\omega_s - \omega_p$
ω_s (reflected)- $\perp$ + $\parallel$	$2\omega_s - \omega_p$	ω_p	ω_p	$2\omega_s - \omega_p$

Table 4. Frequencies generated in each port for cross-polarized, counter propagating pumps, $\omega_p > \omega_s$; grating due to counter-propagating signal and pump. The signal is assumed to have arbitrary polarization. Frequencies shown in green satisfy phase matching condition

	Grating due to reflected ω_s & co-propagating ω_p **Forward**: Grating vector: $k_p + k_s$		**Grating due to co-prop ω_s & counter propagating ω_p** **Backward**: Grating vector: $k_p + k_s$	
	Port 1	Port 2	Port 1	Port 2
ω_p (co-prop)-$\parallel$	ω_s	$2\omega_p - \omega_s$	$2\omega_p - \omega_s$ ($\parallel$)	ω_s
ω_p (reflected)-$\perp$	ω_s	$2\omega_p - \omega_s$	$2\omega_p - \omega_s$ ($\perp$)	ω_s
ω_p (counter-prop)- $\perp$	ω_s	$2\omega_p - \omega_s$ ($\perp$)	$2\omega_p - \omega_s$	ω_s
ω_p (reflected)- $\parallel$	ω_s	$2\omega_p - \omega_s$ ($\parallel$)	$2\omega_p - \omega_s$	ω_s
ω_s (co-prop)- $\perp$ + $\parallel$	$2\omega_s - \omega_p$	ω_p	ω_p	$2\omega_s - \omega_p$
ω_s (reflected)- $\perp$ + $\parallel$	$2\omega_s - \omega_p$	ω_p	ω_p	$2\omega_s - \omega_p$

and counter-propagating pump (backward propagating grating with grating vector, $k_p - k_s$). On the other hand in port 2, polarization-insensitive conjugate generation is due to the grating formed between co-propagating signal and co-propagating pump (forward propagating grating with grating vector $k_p - k_s$) as shown in Table. 3. Thus, conjugate in both polarizations do get generated in ports 1 and 2, but the processes leading to the polarization-insensitive phase conjugation are different for positive and negative detuning. The strength of these gratings and the corresponding phase matching conditions are different and hence detuning performance in port 1 and port 2 are also expected to be different. In this analysis, we neglect the polarization dependent gain of the SOA.

3. Experimental setup, results and discussions

3.1. Detuning characteristics

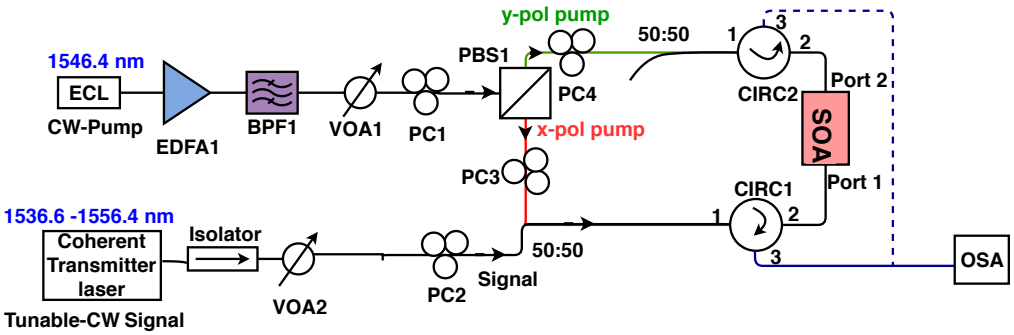

Fig. 4. Schematic of the experimental setup to study the detuning performance of conjugate at ports 1 and 2 of SOA, with tunable CW signal and orthogonally polarized counter-propagating pumps

The schematic of the experimental setup to investigate the detuning characteristics of the Bragg-scattering based FWM in SOA for phase conjugate generation is shown in Fig. 4. Continuous wave signal and cross-polarized counter-propagating pumps are used in this experiment. The pump wavelength is fixed at 1546.4 nm and the signal wavelength is swept in steps of 0.02 nm over a span of 20 nm about pump wavelength using a tunable laser. The pump power is amplified using an erbium doped fiber amplifier (EDFA). The out-of-band amplified spontaneous emission noise from the EDFA is filtered using a band pass filter (BPF).

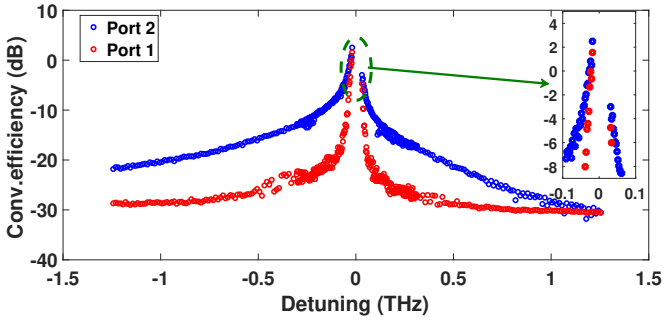

Fig. 5. Conversion efficiency of the conjugate at port 1 and port 2 of the SOA; the detuning region over which the efficiency go below -5 dB is shown in the inset, which can be attributed to the Bragg scattering region.

Output of the pump laser after proper amplification is split into orthogonal polarizations using a polarization beam splitter (PBS) and are counter propagated through a nonlinear SOA, operated at an injection current of 375 mA. The signal is coupled along with the X-polarized pump to the input of SOA through port 1. The additional 50:50 coupler in the Y-polarized arm, on the input side is used to equalize the pump powers in both the polarizations. Note that $\parallel$ polarization is marked as x-pol and $\perp$ polarization is marked as y-pol in this figure. The variable optical attenuator (VOA1) in the pump arm is used to adjust the power levels of the pump in each polarization launched into the SOA, to be 1 dBm. VOA2 in the signal arm is used to adjust the input signal power to be -8 dBm. The pump power is chosen such that it is larger than the

Optics EXPRESS

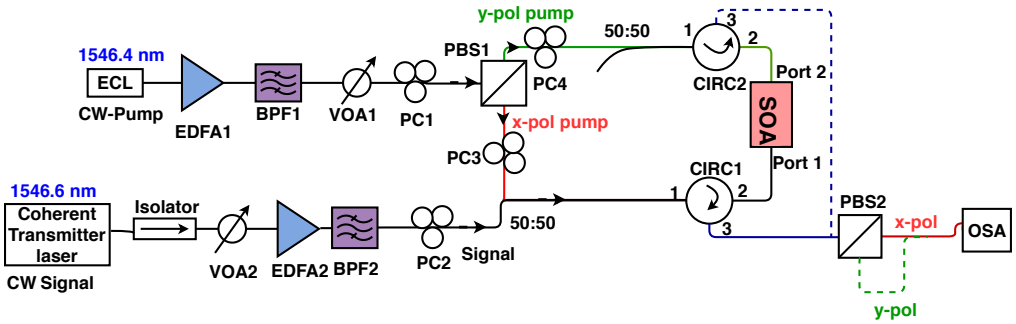

Fig. 6. Schematic of the experimental setup to demonstrate polarization-insensitive phase conjugate generation with CW signal and orthogonally polarized counter-propagating pumps

saturation power of the SOA. Polarization controllers (PCs) are used at different stages in order to ensure the desired state of polarization at the respective stage. Circulators (CIRC) are used in both input and output ports of the SOA to extract power at the respective ports. The spectra at the input and output ports (port 1 and port 2 respectively) are recorded in an OSA (NRT-8000) for different values of detuning between pump and signal.

The variation of conversion efficiency (defined as the ratio of conjugate power to that of the input signal power) with detuning ($\omega_s - \omega_p$) is shown in Fig. 5. The conversion efficiency of the conjugate generated in both the ports of SOA for detuning < 100 GHz is shown in the inset of the Fig. 5. It is evident from Fig. 5 that the efficiency observed in both the ports for the smaller values of detuning are almost identical; while the efficiency reduces to less than 0 dB (<100%) for a detuning of >30 GHz. The particular narrow detuning performance is attributed to the phase mismatch factor for Bragg-scattering phenomena which is explained in Section 2, Fig. 3. The relatively larger conversion efficiency observed in port 2 for larger values of detuning is due to the generation of conjugate through the conventional four wave mixing process occurring due to population pulsations.

3.2. *Demonstration of polarization-insensitive phase conjugate generation*

In order to demonstrate the polarization-insensitive operation in both the ports of SOA, 25 GHz detuning is used with pump wavelength at 1546.4 nm and the signal at 1546.6 nm ($\omega_p > \omega_s$). The corresponding experimental setup is shown in Fig. 6. The description is almost identical to that in Fig. 4, except that, we use a polarization beam splitter (PBS2) at the output side (at port 3 of the CIRC1/2) so that the generated x-polarized and y-polarized conjugates can be observed independently in the OSA. An additional EDFA and a BPF are introduced in the signal arm in order to control the input signal power. Figure. 7(a) shows the spectra of the input signal and those observed at port 1 and port 2 of the SOA. The conversion efficiency is found to be consistent with the detuning performance shown in Fig. 5. At port 2, the efficiency is > 0 dB while at port 1 it is ≈ -2 dB as observed in Fig. 7(a). PC2 in the experimental setup in Fig. 6 is used to adjust the CW input signal to be equally distributed in both the polarizations. As indicated in Fig. 7(b) & 7(c), the conjugates in port 1 and 2 have an almost equal proportion of power in x and y polarizations, as predicted by the theory. This occurs so long as the input signal has equal content in both polarizations. In case the input signal power has an unequal proportion of powers in the x and y polarizations, the phase conjugation would lead to a polarization dependent loss (PDL). In case of the polarization multiplexed coherent communication systems, the corresponding PDL can be corrected by digital signal processing [31].

Even though the detuning used in this experiment is ~25 GHz, the experiment can be performed for larger detuning, with a corresponding trade-off in the conversion efficiency. Demonstrations

Optics EXPRESS

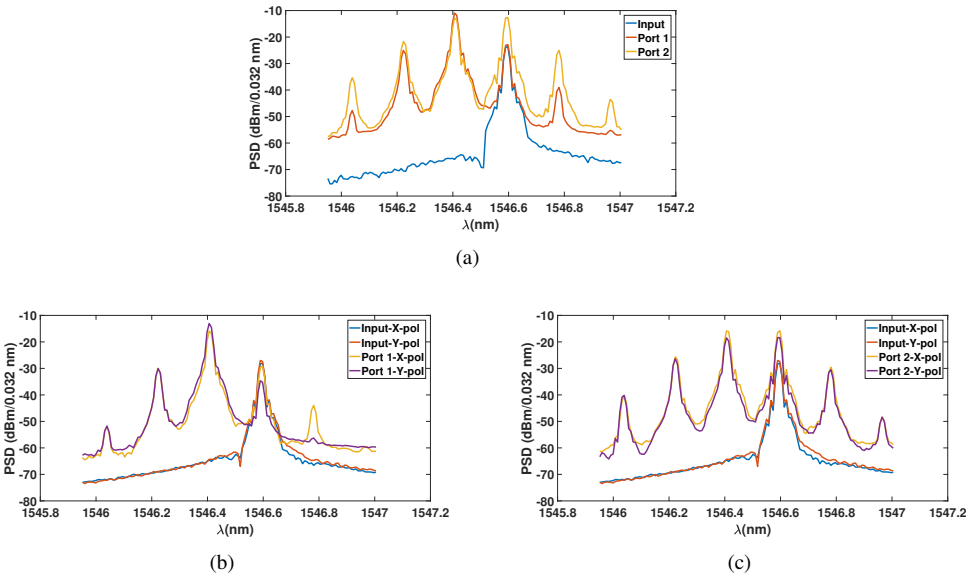

Fig. 7. (a) Spectra of input signal, and output of SOA observed at Port 1 and Port 2. Input and output spectra, demonstrating polarization-insensitive phase conjugate generation of CW signal (b) at port 1 and (c) at port 2 of SOA

of polarization-insensitive phase conjugation in the proposed scheme with data modulated with PM-QPSK and PM-16QAM are performed successfully and the details of these experimental results are being reported elsewhere.

4. Conclusion

Polarization-insensitive phase conjugate generation using counter propagating orthogonally polarized pumps is theoretically explained using the Bragg scattering FWM due to propagating gratings in SOAs. Unlike the conventionally described FWM due to population pulsations, it is critical to consider the phase matching conditions, which in-turn decides the detuning performance in Bragg scattering-based FWM. The generation of the conjugate in both front and back facets of the SOA, their corresponding polarizations along with the appropriate phase matching conditions are explained in detail. It is evident from our analysis that, non-zero facet reflectivity is essential to achieve polarization-insensitive conjugate generation for both positive and negative detuning, in both the ports of the SOA. Experiments are performed to validate the proposed polarization-insensitive phase conjugation generation. The detuning performance is highly limited by the wave-number mismatch. The conversion efficiency of > -10 dB is observed for a detuning range of up to ± 100 GHz in both the front and back facets of the SOA, for both the polarizations. These results would prove to be useful for compact, efficient and flexible phase conjugation generation for polarization multiplexed data in advanced modulation formats.

5. Appendix A

The wave vectors corresponding to pump, signal, idler/conjugate and the moving grating (k_p, k_s, $k_{i/c}$, and ($k_p - k_s$ / $k_p + k_s$)) and the phase mismatch for each scattering process is shown in Fig. 8 for $\omega_p > \omega_s$. Since $\omega_p > \omega_s$, the grating vectors move in the direction of the pump. When the pump and signal co-propagate, the moving grating is generated with a grating vector $k_p - k_s$, while for counter-propagation, the grating is generated with vector $k_p + k_s$. The magnitudes of

Optics EXPRESS

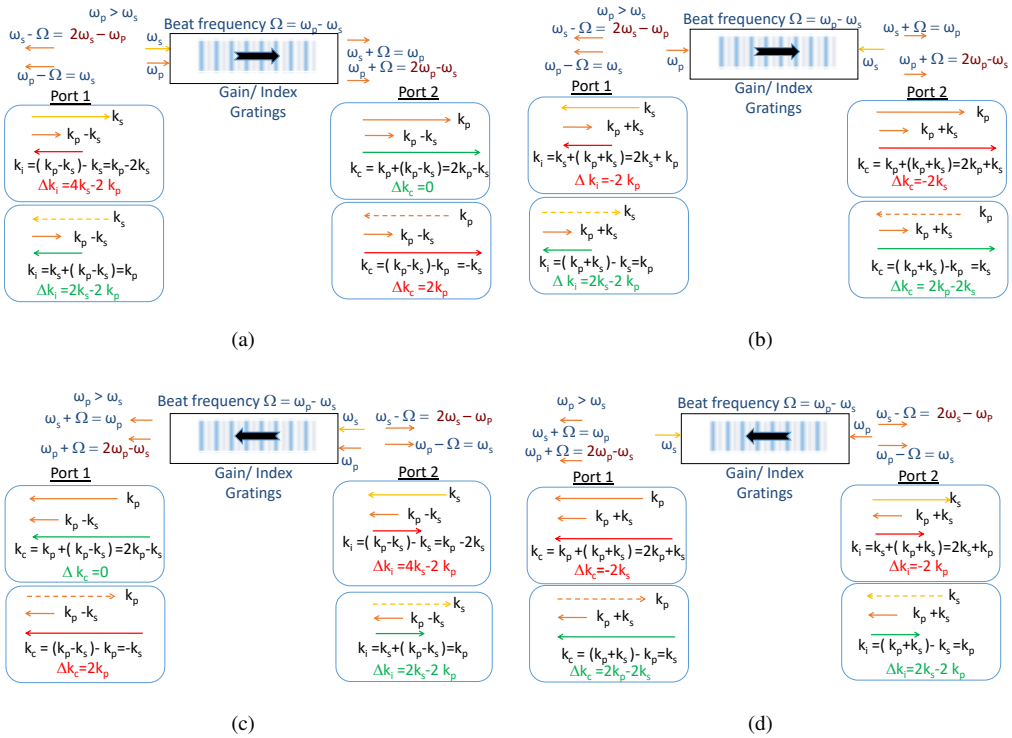

Fig. 8. Forward and backward propagating grating formation and the forbidden (red) and non-forbidden (green) idler/conjugate at port 1 and port 2 of SOA based on phase matching condition for $\omega_p > \omega_s$. The reflected signal and pump from the SOA facets are indicated with dotted lines. (a) Forward propagating grating formed by the beating between co-propagating signal and pump launched from port1. (b) Forward propagating grating formed by the beating between counter-propagating signal and co-propagating pump. (c) Backward propagating grating formed by the beating between co-propagating signal and pump launched from port 2. (d) Backward propagating grating formed by the beating between counter-propagating pump and co-propagating signal

all the grating vectors are decided by the detuning between the signal and the pump.

Funding

Department of Science and Technology (DST)-Govt of India, Office of PSA-Govt of India and Visvesvaraya Ph.D. Scheme of DeitY-Govt of India.

Acknowledgments

Authors would like to acknowledge Dr. Pascal Landais, DCU, Ireland, Krithika V.R for discussions. Authors also acknowledge the unnamed reviewer for valuable suggestions.

References

1. K. Solis-Trapala, T. Inoue, and S. Namiki, "Nearly-ideal optical phase conjugation based nonlinear compensation system," in "Optical Fiber Communication Conference" (Optical Society of America, 2014), paper W3F.8.
2. M. A. Al-Khateeb, M. A. Iqbal, M. Tan, A. Ali, M. McCarthy, P. Harper, and A. D. Ellis, "Analysis of the nonlinear kerr effects in optical transmission systems that deploy optical phase conjugation," Opt. Express **26**(3), 3145–3160 (2018).
3. M. Ding, A. Wonfor, Q. Cheng, R. V. Penty, and I. H. White, "Hybrid MZI-SOA InGaAs/InP photonic integrated switches," IEEE J. Sel. Top. Quantum Electron. **24**(1), 1–8 (2018).

Optics EXPRESS

4. R. S. Tucker and K. Hinton, "Energy consumption and energy density in optical and electronic signal processing," IEEE Photon. J. **3**(5), 821–833 (2011).
5. J. Lacey, S. Madden, and M. Summerfield, "Four-channel polarization-insensitive optically transparent wavelength converter," IEEE Photon. Technol. Lett. **9**(10), 1355–1357 (1997).
6. U. Feiste, R. Ludwig, E. Dietrich, S. Diez, H. Ehrke, D. Razic, and H. Weber, "40 gbit/s transmission over 434 km standard fibre using polarisation independent mid-span spectral inversion," Electron. Lett. **34**(21), 2044–2045 (1998).
7. J. P. Lacey, M. A. Summerfield, and S. Madden, "Tunability of polarization-insensitive wavelength converters based on four-wave mixing in semiconductor optical amplifiers," J. Lightwave Technol. **16**(12), 2419–2427 (1998).
8. K. Inoue, "Spectral inversion with no wavelength shift based on four-wave mixing with orthogonal pump beams," Opt. Lett. **22**(23), 1772–1774 (1997).
9. A. Mecozzi, G. Contestabile, F. Martelli, L. Graziani, A. D'Ottavi, P. Spano, R. Dall'Ara, J. Eckner, F. Girardin, and G. Guekos, "Optical spectral inversion without frequency shift by four-wave mixing using two pumps with orthogonal polarization," IEEE Photon. Technol. Lett. **10**(3), 355–357 (1998).
10. I. Zacharopoulos, I. Tomkos, D. Syvridis, T. Sphicopoulos, C. Caroubalos, and E. Roditi, "Study of polarization-insensitive wave mixing in bulk semiconductor optical amplifiers," IEEE Photon. Technol. Lett. **10**(3), 352–354 (1998).
11. C. Greco, F. Martelli, A. D'Ottavi, A. Mecozzi, P. Spano, and R. Dall'Ara, "Frequency-conversion efficiency independent of signal-polarization and conversion-interval using four-wave mixing in semiconductor optical amplifiers," IEEE Photon. Technol. Lett. **11**(6), 656–658 (1999).
12. J. Tang and K. A. Shore, "A simple scheme for polarization insensitive four-wave mixing in semiconductor optical amplifiers," IEEE Photon. Technol. Lett. **11**(9), 1123–1125 (1999).
13. J. Tang, P. S. Spencer, and K. A. Shore, "Practical scheme for polarization-insensitive and frequency-conversion interval–independent four-wave mixing in semiconductor optical amplifiers," Opt. Lett. **24**(22), 1605–1607 (1999).
14. J. Tang, P. S. Spencer, and K. A. Shore, "Efficient polarization insensitive four-wave mixing using a semiconductor optical amplifier and one pump source in an optical loop," Appl. Phys. Lett. **75**(18), 2710–2712 (1999).
15. J. Tang, P. S. Spencer, and K. A. Shore, "Enhanced performance of polarization-independent four-wave mixing in polarization-sensitive semiconductor optical amplifiers," IEEE Photon. Technol. Lett. **13**(5), 496–498 (2001).
16. Y. Hong, S. Bandyopadhyay, P. S. Spencer, and K. A. Shore, "Polarization-independent optical spectral inversion without frequency shift using a single semiconductor optical amplifier," IEEE J. Quantum Electron. **39**(9), 1123–1128 (2003).
17. S. Bandyopadhyay, Y. Hong, P. S. Spencer, and K. A. Shore, "Simple techniques for highly efficient wavelength conversion with low polarization sensitivity by use of semiconductor optical amplifiers," J. Opt. Soc. Am. B **21**(5), 1023–1031 (2004).
18. Y. Hong, P. S. Spencer, and K. A. Shore, "Wide-band polarization-free wavelength conversion based on four-wave-mixing in semiconductor optical amplifiers," IEEE J. Quantum Electron. **40**(2), 152–156 (2004).
19. C. Janer and M. Connelly, "Optical phase conjugation technique using four-wave mixing in semiconductor optical amplifier," Electron. Lett. **47**(12), 716–717 (2011).
20. A. Anchal, K. P. Kumar, S. O'Duill, P. M. Anandarajah, and P. Landais, "Experimental demonstration of optical phase conjugation using counter-propagating dual pumped four-wave mixing in semiconductor optical amplifier," Opt. Commun. **369**, 106–110 (2016).
21. D. Méchin, R. Provo, J. Harvey, and C. McKinstrie, "180-nm wavelength conversion based on Bragg scattering in an optical fiber," Opt. Express **14**(20), 8995–8999 (2006).
22. H. McGuinness, M. Raymer, C. McKinstrie, and S. Radic, "Wavelength translation across 210 nm in the visible using vector Bragg scattering in a birefringent photonic crystal fiber," IEEE Photon. Technol. Lett. **23**(2), 109–111 (2011).
23. Y. Zhao, P. Donvalkar, and A. L. Gaeta, "Telecom-to-near-visible frequency translation via Bragg scattering four-wave mixing in a Rb vapor cell," in "CLEO: Science and Innovations," (Optical Society of America, 2017), paper JTu5A.32.
24. Y. Zhao, D. Lombardo, J. Mathews, and I. Agha, "All-optical switching via four-wave mixing Bragg scattering in a silicon platform," APL Photonics **2**(2), 026102 (2017).
25. P. S. Donvalkar, V. Venkataraman, S. Clemmen, K. Saha, and A. L. Gaeta, "Frequency translation via four-wave mixing Bragg scattering in rb filled photonic bandgap fibers," Opt. Lett. **39**(6), 1557–1560 (2014).
26. S. Aneesh, V. Krithika, and D. Venkitesh, "Counter-propagating cross-polarized pumps for efficient conjugate generation using FWM in SOA," in "Australian Conference on Optical Fibre Technology," (Optical Society of America, 2016), paper JT4A.16.
27. B. W. Hakki, and T. L. Paoli, "cw degradation at 300^0 K of GaAs double-heterostructure junction lasers. II. Electronic gain," J. Appl. Phys. **44**(9), 4113–4119 (1973).
28. G. P. Agrawal, "Population pulsations and nondegenerate four-wave mixing in semiconductor lasers and amplifiers," J. Opt. Soc. Am. B **5**(1), 147–159 (1988).
29. G. P. Agrawal and N. A. Olsson, "Self-phase modulation and spectral broadening of optical pulses in semiconductor laser amplifiers," IEEE J. Quantum Electron. **25**(11), 2297–2306 (1989).
30. A. Mecozzi, "Analytical theory of four-wave mixing in semiconductor amplifiers," Opt. Lett. **19**(12), 892–894 (1994).
31. J. Zhou, G. Zheng, and J. Wu, "Constant Modulus Algorithm With Reduced Probability of Singularity Enabled by PDL Mitigation," J. Lightwave Technol. **35**(13), 2685–2694 (2017).